Geometric Optical Investigation of the Underwater Visual Field of Aerial Animals

GÁBOR HORVÁTH
Central Research Institute for Physics of the Hungarian Academy of Sciences, Biophysical Group, H-1525 Budapest, P.O.B. 49, Hungary

AND

DEZSŐ VARJÚ
Lehrstuhl für Biokybernetik, Universität Tübingen, D-7400 Tübingen 1, Federal Republic of Germany

Received 15 October 1989; revised 14 May 1990

ABSTRACT

The underwater visual field distorted by refraction for aerial animals living near the water surface is investigated by means of geometric optics. The imaging of underwater objects by one and two aerial eyes is studied. The underwater binocular image field is determined for pairs of aerial eyes placed in horizontal and vertical planes. Some possible biooptical consequences of the visual detection of underwater prey and predator by aerial animals are discussed on the basis of the structure of their distorted visual field.

INTRODUCTION

It is a well-known phenomenon that the apparent position of an underwater object viewed from the air does not coincide with its true position because of the refraction of light at the water surface [1, 2]. This distortion can be experienced in everyday life, when we view the underwater world as we fish or boat or when we gaze at the aquatic world in the aquarium, for example.

The correct relationship between the apparent and true positions of underwater prey or predator is of particular importance for certain terrestrial animals living near the air-water interface. It is not all the same to a seal, for example, whether one of its companions or one of its main predators, a polar bear, approaches under water. It is important for the mother seals, too, that from the coast they can visually follow their pups swimming in the water [3–5].

 0025-5564/90/$03.50

A polar bear attacking a seal that has just crawled out of an ice-hole has to cope with the modification of the optical information due to refraction. A brown bear fishing in a mountain creek must take into account the difference between the true and apparent positions of the trout in order to successfully capture it.

Fish-eating (piscivorous) birds must not neglect the distortion due to refraction during fishing [6–12]. Insects living on the water surface, for example, waterstriders (Gerridae), have to cope with refraction to catch aquatic prey or to flee from an underwater predator [13, 14].

In spite of the fact that large numbers of animals find their food in the water, or must fear the attack of an underwater predator, it has been proved with only a few animals that refraction is taken into account during prey capture. Recently the ability to correct for refraction was demonstrated in a western reef heron, *Egretta gularis schistacea* [6, 7].

The underwater visual field distorted by refraction for aerial animals, their astigmatic imaging of underwater objects viewed by one and two eyes, and the effect of the distorted structure of the image field on the catching of aquatic prey or recognition of underwater predators is treated in this work. The problem of aquatic animals viewing aerial objects is treated elsewhere [15].

IMAGING OF UNDERWATER OBJECTS WITH ONE AERIAL EYE

Consider an underwater object point O in the system of coordinates of Figure 1. From O a bundle of rays of light radiate toward the water surface in a cone with aperture half-angle $\alpha_t = \arcsin(1/n)$ (angle of total reflection), where n is the index of refraction of water. The surface formed by the refracted rays extrapolated backwards is called the caustic surface. The area between the caustic surface and the water surface is the image area (IA), since it is within this area that the refracted rays extrapolated backwards intersect.

The peak of the IA and the origin of the system of coordinates are the points A and C, respectively. At every point of the IA, two refracted rays extrapolated backwards intersect (see point E in Figure 1, for example). All the rays on a cone intersect at a point of the line $\overline{AC}$ (see point D in Figure 1, for example).

Consider that homocentric, narrow bundle of rays of light proceeding from the underwater point O, which passes through the pupil of the lens eye of an aerial animal. When this bundle is incident at the water surface, it is refracted into a system of rays that is not homocentric; an astigmatic bundle of refracted rays is obtained. Figure 2 represents the main section of this astigmatic refracted pupil bundle. The boundary rays cut a body

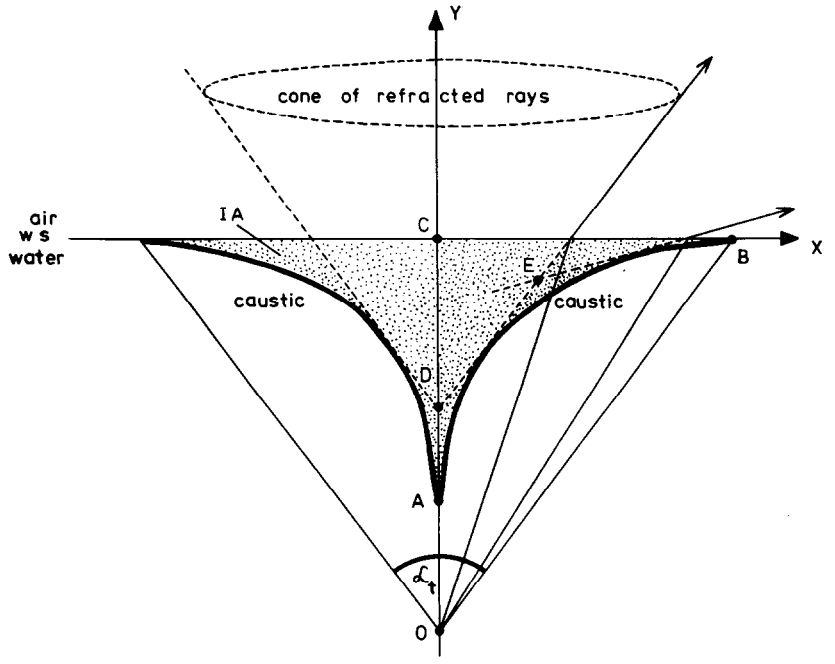

FIG. 1. An underwater bundle of rays of light starting from O with aperture half-angle $\alpha_t = \arcsin(1/n)$, the evolute of the refracted rays extrapolated backwards (caustic) and the image area (IA, dotted); ws, water surface.

from the IA. This slender, wedge-shaped body (dotted) is called the astigmatic image body (AIB) of the object point O, and it can be seen in Figure 3. The points on the caustic are labeled D_1, D_4, D_3, D_5, and the edge on the y axis, I_1I_3. Consider a segment of a cone of rays that crosses the pupil (see arc $S_4S_2S_5$ in Figure 2, for example). The rays extrapolated backwards will pass through a point of the edge I_1I_3. Consequently, a considerable number of rays contribute to the image of every edge point on I_1I_3. The longest pupil arc $S_4S_2S_5$ passes through the center S_2 of the pupil, and the length of the pupil arcs decreases with increasing distance from S_2.

The brightness of an image point is proportional to the number of rays constructing it. Therefore the brightest point on the edge I_1I_3 is I_2, belonging to the pupil arc $S_4S_2S_5$. The brightness of an edge point on I_1I_3 is proportional to the length l of the pupil arc belonging to this point.

If the intensity of the brightest edge point I_2 is i_{max}, and the length of the pupil arc $S_4S_2S_5$ belonging to I_2 is l_{max}, the intensity of an edge point

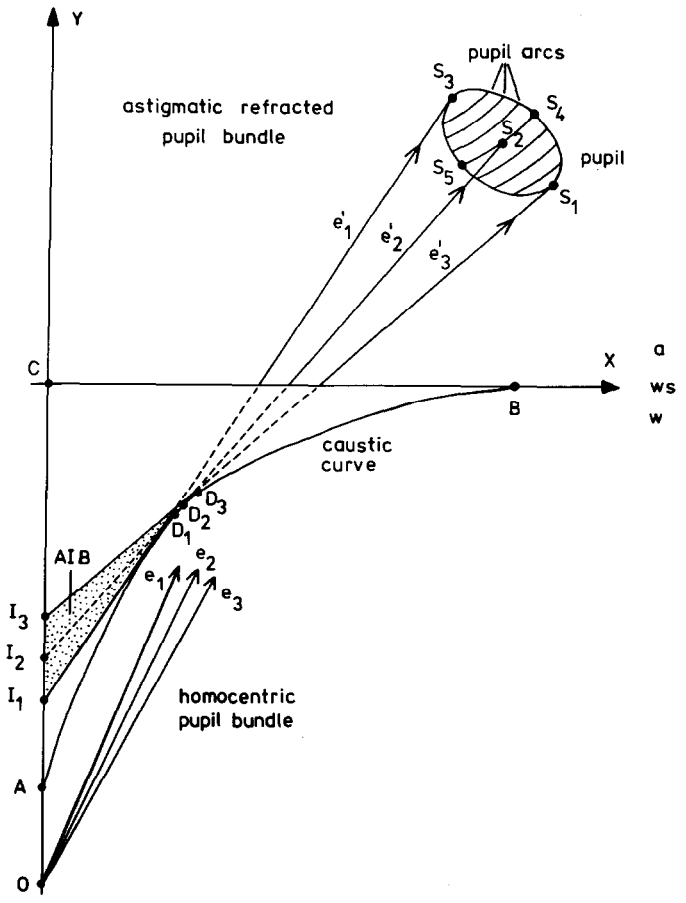

FIG. 2. The main section of the underwater homocentric and the aerial astigmatic refracted pupil bundle passing through the pupil of the lens eye of an aerial animal. AIB, astigmatic image body (dotted); a, air; ws, water surface; w, water.

can be expressed by

$$i = i_{max} l / l_{max}. \tag{1}$$

Figure 4a shows the shape of the AIB in the case of a nearly circular pupil, when $\overline{S_4S_5} \approx \overline{S_1S_3}$. The AIB is vertically and horizontally flattened on its edge and back, respectively. In Figure 4b the shape of the AIB can be seen for a vertically elongated pupil ($\overline{S_4S_5} \ll \overline{S_1S_3}$). Almost the entire AIB is flattened in the vertical plane; it has a very narrow horizontally flattened

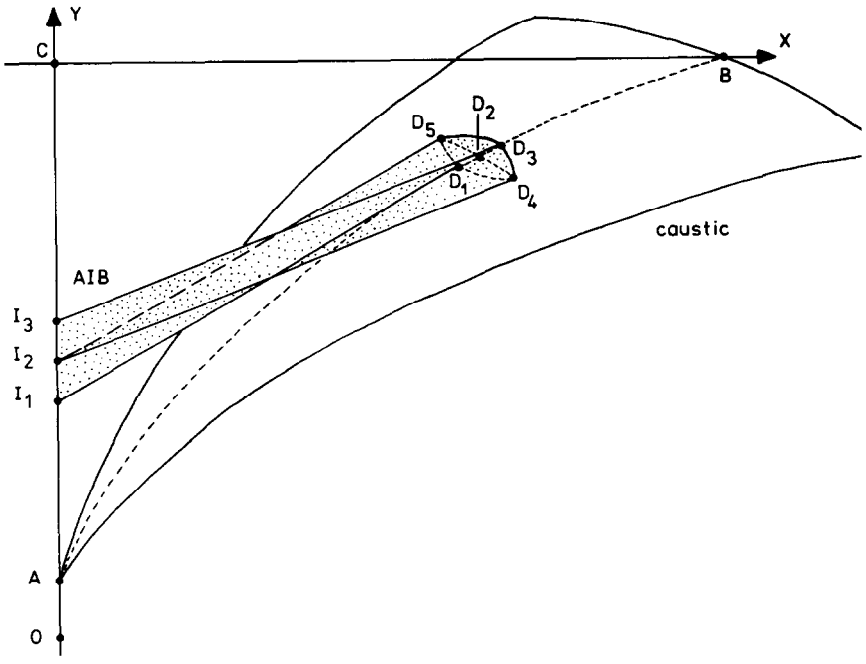

FIG. 3. The wedge-shaped astigmatic image body (AIB, dotted) is the astigmatic image of the underwater object point O. The AIB is constructed by the rays of the astigmatic refracted pupil bundle extrapolated backwards.

back, and it becomes the triangle $I_1I_3D_3$ as $\overline{S_4S_5} \to 0$. When the pupil is horizontally elongated ($\overline{S_4S_5} \gg \overline{S_1S_3}$), almost the entire AIB is flattened in an oblique plane; its vertically flattened edge part is very slender. In this case the AIB becomes the triangle $I_2D_4D_5$ as $\overline{S_1S_3} \to 0$.

Using Equation (1), the following can be deduced. In the case of a horizontally elongated pupil, the edge point I_2 and its very small surroundings on the edge have a high intensity in comparison with the other edge points. When the pupil is circular, the highlighted area surrounding I_2 is larger, and it extends to almost the entire edge in the case of the vertically elongated pupil. Therefore we conclude that when the pupil is horizontally elongated, the most highlighted part of the AIB is almost limited to the edge point I_2, which is the image of an underwater object point O. If the pupil is circular, the most highlighted part of the AIB extends to almost its entire edge, so that the image of O is the line $\overline{I_1I_3}$. The other points of the AIB have such low intensities that they do not play any role in the image construction when the pupil is circular or horizontally elongated. Thus the AIB without its edge can be called the imperceptible astigmatic phantom

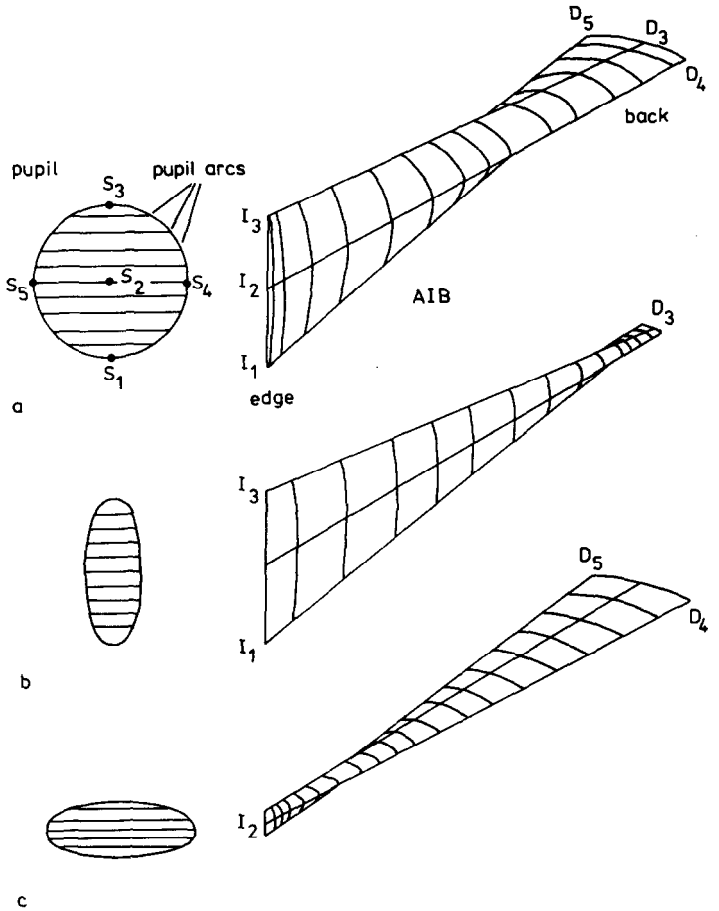

FIG. 4. The shape of the AIB for differently shaped pupils. (a) A circular pupil; (b) vertically and (c) horizontally elongated pupils.

image of O. In the case of a vertically elongated, very narrow pupil, the most highlighted part of the AIB is again its edge, but the difference between the brightness of the edge and that of the other points is not very large. Therefore, in this case the astigmatic phantom image is dimly perceptible, and it could influence the sharpness of the aerial image of underwater objects.

BINOCULAR IMAGING OF UNDERWATER OBJECTS

In general the diameter of the pupil can be neglected in comparison with the distance between the eyes of an aerial animal and an underwater

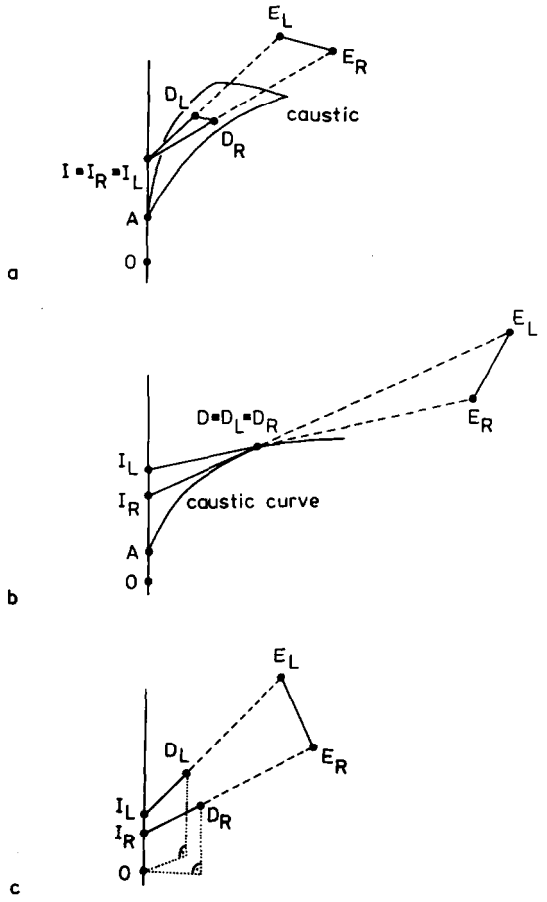

FIG. 5. (a) When the right and left eyes E_R and E_L of an aerial animal lie in a horizontal plane, the astigmatic image lines $\overline{I_R D_R}$ and $\overline{I_L D_L}$ intersect in the point $I_R \equiv I_L \equiv I$, so that the binocular ordinary image point of O is I. (b) When the eyes and the object point O lie in the same vertical plane, the astigmatic image lines intersect in the point $D_R \equiv D_L \equiv D$, and therefore the binocular extraordinary image point of O is D. (c) In any other case the astigmatic image lines have no common point, so no binocular image point exists.

object viewed by it; therefore the AIB is very slender, and it can be approximated by an image line $\overline{ID}$, which extends from the edge (I) to the back (D). Binocular vision results in at least two definite, unique image positions. When a pointlike light source is viewed with the eyes in a horizontal plane, the two bundles of rays entering the eyes appear to come from I (Figure 5a), but when the eyes and the object point O lie in a vertical plane, the two bundles of rays appear to come from D (Figure 5b).

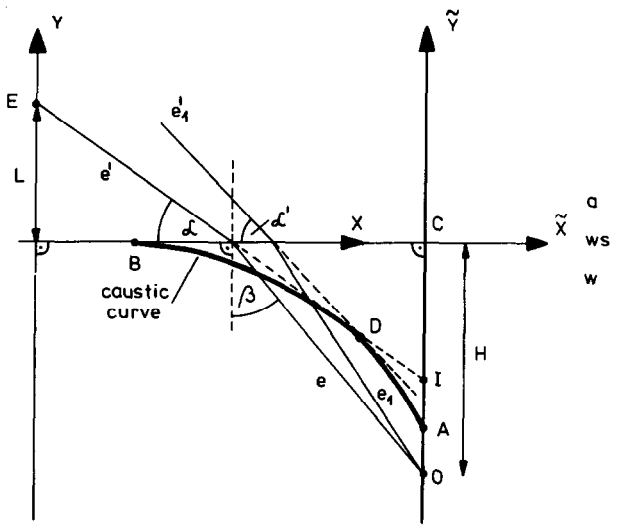

FIG. 6. The determination of the underwater binocular ordinary and extraordinary image fields (UBOIF and UBEIF). The binocular ordinary and extraordinary images of O are I and D, respectively; the eyes of an aerial animal are placed on the y axis at distance L from the water surface.

In any other case there is no binocular image point, because the two bundles of rays entering the eyes do not intersect; that is to say, the astigmatic image lines for the right and left eyes have no common point (Figure 5c, cf. also [2]).

Since objects are usually viewed with both eyes lying in a horizontal plane, the customary binocular image point of an underwater object point O is I. In this case the image of the underwater world is determined by these points I, and the image field they constitute is called in this work the underwater binocular ordinary image field (UBOIF). The space determined by the points D is called the underwater binocular extraordinary image field (UBEIF); it is the binocular image of the underwater world when the eyes lie on a vertical line. In the following we determine the caustic curve, the UBOIF, and the UBEIF for a grid of underwater object points.

THE CAUSTIC CURVE

The caustic is determined by the extraordinary image points D of an underwater object point. Let two rays of light e and e_1 (Figure 6) start out in a vertical plane from the underwater object point $O = (\tilde{x} = 0, \tilde{y} = -H)$. The angles between the water surface and the refracted rays e' and e_1' are α and α', respectively. The extraordinary image point D of O lies in the

intersection of the lines e' and e_1' extrapolated backwards as $\alpha' \to \alpha$. The equation of the line e' is

$$\tilde{y}_1(\tilde{x}) = -(\tilde{x} + H\tan\beta)\tan\alpha, \tag{2}$$

where $H = \overline{OC}$ and β is the angle between the y axis and the line e. On the basis of the refraction law $\cos\alpha = n\sin\beta$,

$$\tan\beta = \frac{\cos\alpha}{(n^2 - \cos^2\alpha)^{1/2}} \tag{3}$$

follows. From (2) and (3) we obtain

$$\tilde{y}_1(\tilde{x}) = -\left[\tilde{x} + \frac{H\cos\alpha}{(n^2 - \cos^2\alpha)^{1/2}}\right]\tan\alpha. \tag{4}$$

Similarly, the equation of the line e_1' can be obtained as

$$\tilde{y}_2(\tilde{x}) = -\left[\tilde{x} + \frac{H\cos(\alpha + \Delta\alpha)}{[n^2 - \cos^2(\alpha + \Delta\alpha)]^{1/2}}\right]\tan(\alpha + \Delta\alpha), \tag{5}$$

where $\Delta\alpha = \alpha' - \alpha$. If the diameter of the pupil can be neglected in comparison to the distance between the eye and the object viewed by it, then $\Delta\alpha \ll 1$, and therefore the following approximations can be used:

$$\tan(\alpha + \Delta\alpha) \approx \frac{\tan\alpha + \Delta\alpha}{1 - \Delta\alpha\tan\alpha}, \qquad \cos(\alpha + \Delta\alpha) \approx \cos\alpha - \Delta\alpha\sin\alpha. \tag{6}$$

The coordinates $\tilde{x}, \tilde{y}$ of the point D are determined by the equation

$$\tilde{y}_1(\tilde{x}) = \tilde{y}_2(\tilde{x}) \qquad \text{as} \quad \Delta\alpha \to 0. \tag{7}$$

From Equations (4)–(7) we obtain for the $\tilde{x}$ coordinate of D

$$\tilde{x} = -H\cos^2\alpha \lim_{\Delta\alpha \to 0}\left[\frac{\dfrac{(\tan\alpha + \Delta\alpha)(\cos\alpha - \Delta\alpha\sin\alpha)}{[n^2 - (\cos\alpha - \Delta\alpha\sin\alpha)^2]^{1/2}} - \dfrac{\sin\alpha(1 - \Delta\alpha\tan\alpha)}{(n^2 - \cos^2\alpha)^{1/2}}}{\Delta\alpha}\right]. \tag{8}$$

Using L'Hospital's law, making the limit $\Delta\alpha \to 0$, we derive from (4) and (8)

the coordinates of D as a function of α:

$$\tilde{x}(\alpha) = \frac{-H(n^2-1)\cos^3\alpha}{(n^2-\cos^2\alpha)^{3/2}}, \qquad \tilde{y}(\alpha) = -\frac{Hn^2\sin^3\alpha n}{(n^2-\cos^2\alpha)^{3/2}}. \tag{9}$$

Eliminating the angle α from (9), we obtain the function $\tilde{y}_c(\tilde{x})$ of the caustic curve,

$$\tilde{y}_c(\tilde{x}) = -\frac{H}{n}\left[1-(n^2-1)\left(\frac{-x}{H(n^2-1)}\right)^{2/3}\right]^{3/2}. \tag{10}$$

The coordinates of the endpoints A and B of the caustic curve are

$$\underline{A} = (0, -H/n), \qquad \underline{B} = \left[-H(n^2-1)^{-1/2}, 0\right] \tag{11}$$

in the system of coordinates $\tilde{x}, \tilde{y}$ of Figure 6. Analysis of (9) reveals that the extraordinary image point D moves along the caustic curve from the point A towards B as α decreases from $\pi/2$ to zero.

Since the caustic is the evolute of the refracted rays extrapolated backwards, the coordinate $\tilde{x}$ can be determined from the disappearance of the partial differential quotient $\partial\tilde{y}_1/\partial\alpha$, too. From (4), it follows that

$$\frac{\partial\tilde{y}_1}{\partial\alpha} = \frac{-\tilde{x}}{\cos^2\alpha} - H\cos\alpha\frac{n^2-1}{(n^2-\cos^2\alpha)^{3/2}} = 0. \tag{12}$$

From (12) one obtains for $\tilde{x}(\alpha)$ and $\tilde{y}(\alpha)$ the same expression as in (9).

THE UNDERWATER BINOCULAR ORDINARY IMAGE FIELD (UBOIF)

Consider an underwater object point $O(x, y)$ observed by an aerial animal with eyes placed in a horizontal plane in the system of coordinates x, y of Figure 6. The binocular ordinary image of O is the point $I(x, y')$. If a ray e starting from O reaches the eyes E of the animal after refraction (e'), I comes to lie in the intersection of the line e' extrapolated backwards and the vertical line through O, as already shown above.

Let the eyes of the aerial animal be on the y axis at distance L from the water surface. We can write on the basis of Figure 6

$$L\cot\alpha - y\tan\beta = x, \qquad y' = L - x\tan\alpha. \tag{13}$$

From (3) and (13) we obtain

$$F(\tan\alpha) = a_0 + a_1\tan\alpha + a_2\tan^2\alpha + a_3\tan^3\alpha + a_4\tan^4\alpha = 0, \quad (14a)$$

with

$$a_0 = L^2(n^2-1), \quad a_1 = -2Lx(n^2-1), \quad a_2 = n^2(L^2+x^2) - (x^2+y^2),$$

$$a_3 = -2Lxn^2, \quad a_4 = n^2x^2. \quad (14b)$$

The fourth-degree equation (14) can be solved analytically for $\tan\alpha$. However, because of the complexity, it is more expedient to solve them numerically, using the tangent method of Newton, for example, that is, using the following recursion for the approximate roots $(\tan\alpha)_i$ in the

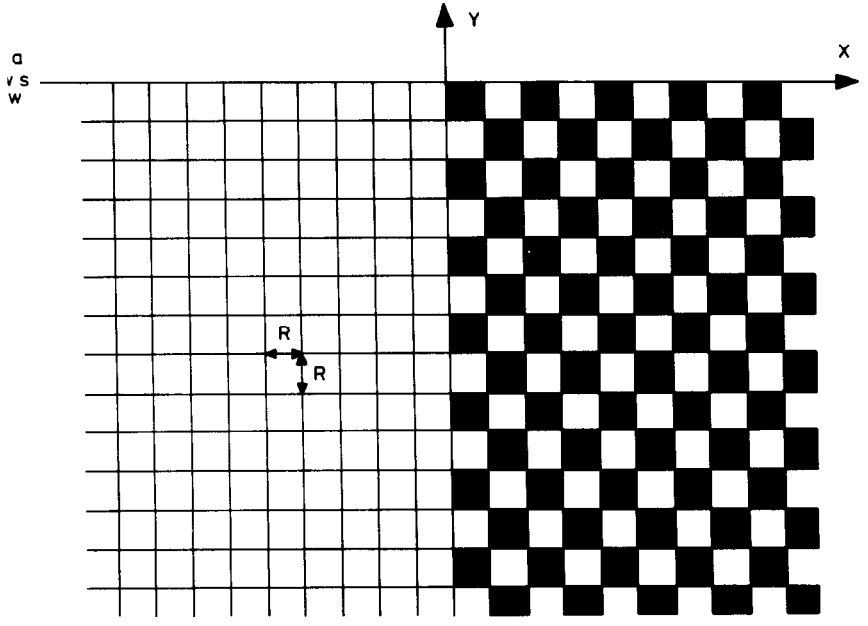

FIG. 7. The two-dimensional vertically oriented quadratic grid with grid parameter R as the underwater object space. For the sake of better visualization, the cells are alternately painted white and black on the right half of the object space.

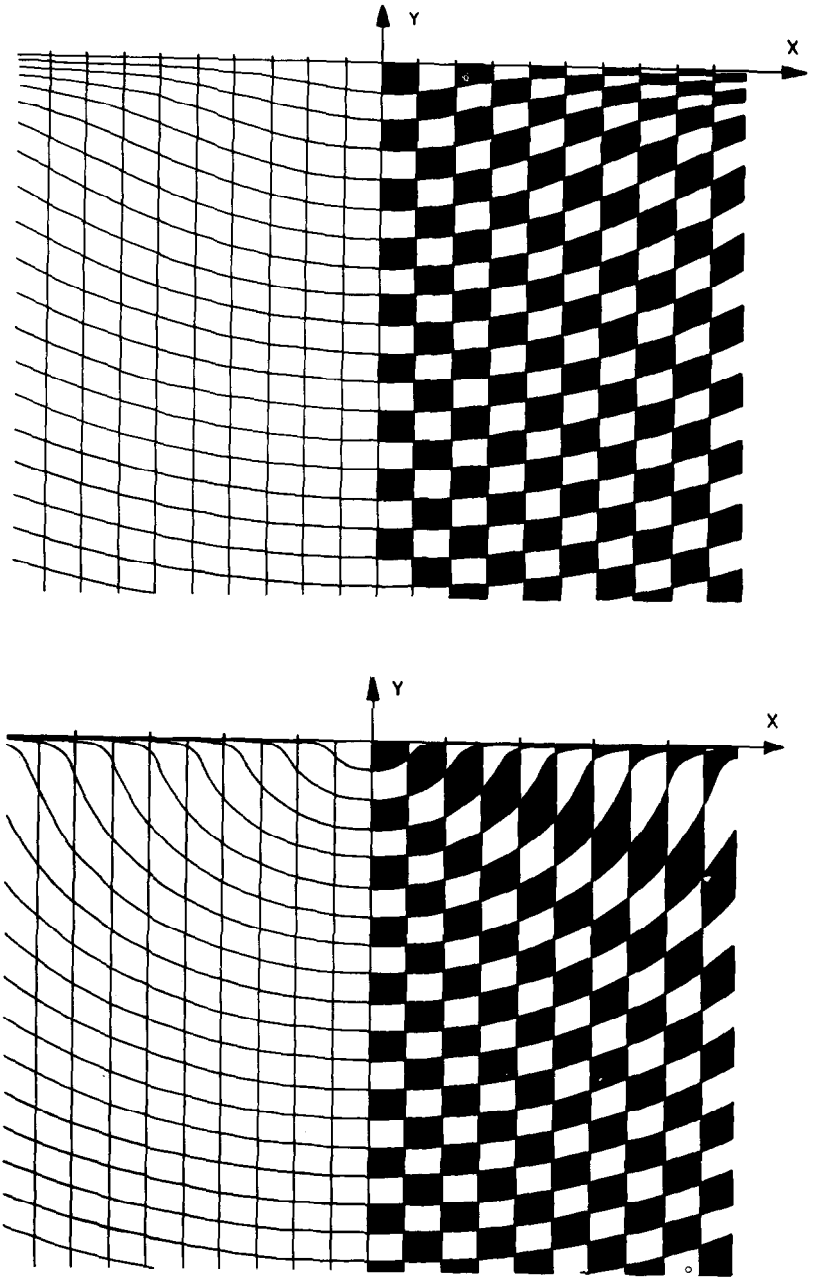

FIG. 8. The underwater binocular ordinary image field (UBOIF). (a) Relative grid parameter $R/L = 1$ (nearspace). The scale on the x axis is L. (b) Relative grid parameter $R/L = 50$ (farspace); scale on the x axis is $100L$.

successive iteration steps:

$$(\tan\alpha)_{i+1} = (\tan\alpha)_i - \frac{F[(\tan\alpha)_i]}{\dot{F}[(\tan\alpha)_i]}, \qquad \dot{F} \equiv \frac{dF}{d(\tan\alpha)}. \tag{15}$$

Solving (14) numerically for $\tan\alpha$ and then using (13), the ordinate y' of the ordinary image point I is obtained.

After these steps we can determine the UBOIF distorted by refraction for an aerial animal. Consider the two-dimensional quadratic grid in a vertical plane (Figure 7) as the underwater object space

$$y = -iR, \qquad x = \pm jR; \qquad i, j = 0, 1, 2, 3, \ldots, \tag{16}$$

where $R > 0$ is the grid parameter. The binocular ordinary images of the vertical lines $x = \pm jR$ are also vertical lines. The binocular ordinary images of the horizontal lines $y = -iR$ can be determined numerically from (13) and (14).

The results can be seen in Figure 8, on which the near and far areas of the UBOIF (called nearspace and farspace) are represented. From (13) and (14), we derive the limits

$$\lim_{x\to 0} y' = -\frac{y}{n}, \qquad \lim_{x\to\infty} y' = 0. \tag{17}$$

THE UNDERWATER BINOCULAR EXTRAORDINARY IMAGE FIELD (UBEIF)

The UBEIF is determined by the extraordinary image points $D(x', y')$ placed on the caustic in the system of coordinates x, y of Figure 6. Using (9), and considering Figure 6,

$$y' = y\frac{n^2\cos^3\alpha}{(n^2 - \sin^2\alpha)^{3/2}}, \tag{18}$$

$$x' = x + y\frac{(n^2-1)\sin^3\alpha}{(n^2 - \sin^2\alpha)^{3/2}}, \tag{19}$$

$$L - y' = x'\cot\alpha \tag{20}$$

follow. Dividing (18) by (19) and then eliminating $\cot\alpha$ from (18)–(20), we obtain

$$x'^3 - x'\frac{n^2(L-y')^3}{(n^2-1)y'} + \frac{xn^2(L-y')^3}{(n^2-1)y'} = 0, \tag{21}$$

and eliminating $\cot\alpha$ from (18) and (20),

$$x'(y', y, L) = (L - y')\left(\frac{n^2 y}{y'}\right)^{1/3}\left[\frac{1 - n^2(y'/n^2 y)^{2/3}}{n^2 - 1}\right]^{1/2}. \quad (22)$$

The function $x'(y', y, L)$ gives the binocular extraordinary image of the horizontal lines (y = constant ≤ 0) of the underwater object field. Using the Cardano formula, we obtain from (21)

$$x'(y', x, L) = \left[-\frac{Q}{2} + \left(\frac{Q^2}{4} + \frac{p^3}{27}\right)^{1/2}\right]^{1/3} + \left[-\frac{Q}{2} - \left(\frac{Q^2}{4} + \frac{p^3}{27}\right)^{1/2}\right]^{1/3},$$

$$p = -\frac{n^2(L - y')^3}{(n^2 - 1)y'}, \qquad Q = -px. \quad (23)$$

The discriminant of the third-degree equation (21) is

$$D = p^2\left[\frac{x^2}{4} + \frac{n^2(L + |y'|)^3}{27(n^2 - 1)|y'|}\right] > 0. \quad (24)$$

Since $D > 0$, (21) has only one real root for x'. The function $x'(y', x, L)$ gives the binocular extraordinary image of the vertical half-lines (x = constant, $y \leq 0$) of the underwater object field.

The functions $x'(x, y)$ and $y'(x, y)$ cannot be determined analytically, so we use further on expressions (22) and (23) to calculate the near and far underwater binocular extraordinary image fields (UBEIFs). They are plotted in Figures 9a and 9b, respectively. In Figures 10 and 11 examples can be seen of the relationship between the UBOIF and the UBEIF. In Figure 10 the slanted lines interconnect the extraordinary and ordinary image points of object points lying on a horizontal line. Similar lines are plotted in Figure 11 for object points along a vertical line.

THE UNDERWATER VISUAL FIELD FOR DIFFERENT ARRANGEMENTS OF EYES

On the basis of Figure 5, the following can be concluded for the underwater visual field in the case of differently arranged eyes of an aerial animal.

(1) When both eyes are placed along a vertical line, a vertical plane can laid through the eyes and any underwater object points. In this case the underwater visual field is the UBEIF (Figure 9).

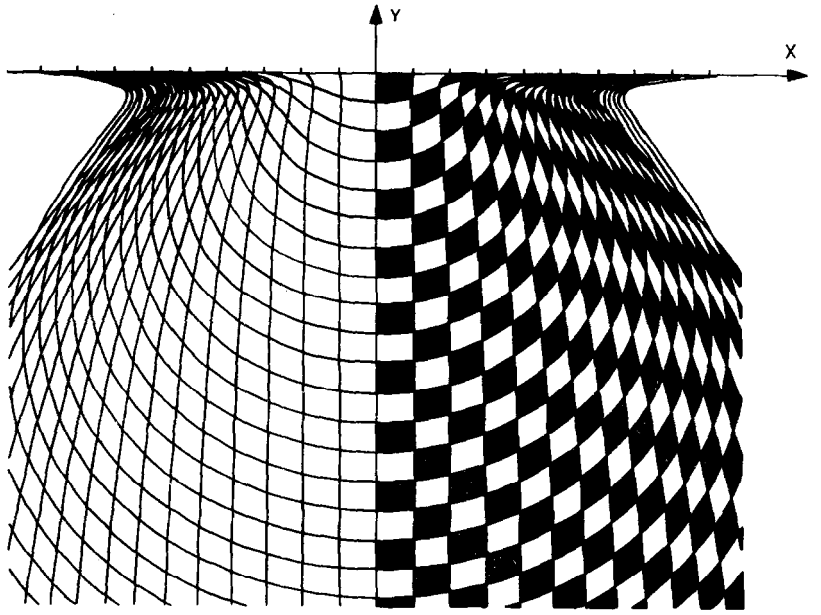

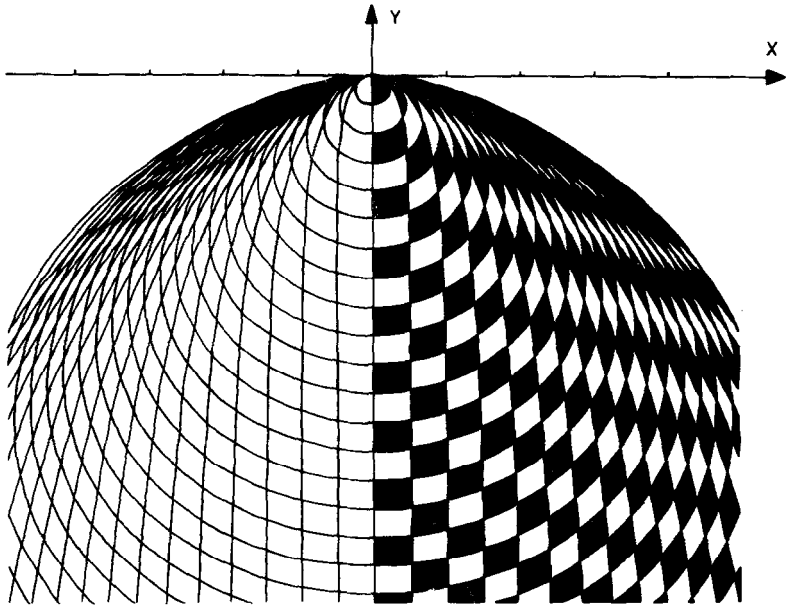

b

FIG. 9. (a) The nearspace of the underwater binocular extraordinary image field UBEIF ($R/L = 1$). (b) The farspace of the UBEIF ($R/L = 50$). Scales as in Figure 8.

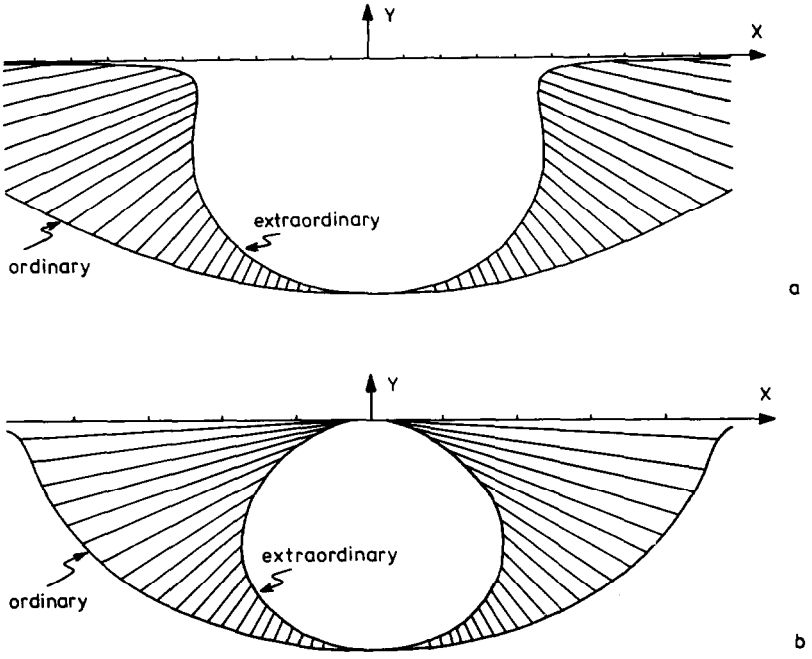

FIG. 10. The relationship between the UBOIF and the UBEIF. The slanted lines interconnect the extraordinary and ordinary image points of object points lying on a horizontal underwater line. (a) $R/L = 1$ (nearspace); (b) $R/L = 50$ (farspace). Scales as in Figure 8.

(2) When the eyes lie in a vertical plane, but not along a vertical line, the image of only those underwater object points that lie in the vertical plane containing both eyes appears in the UBEIF (Figure 9). The underwater object points outside of this vertical plane have no binocular image point.

(3) When the eyes lie in a horizontal plane, the image of the underwater object points in the vertical plane passing through the eyes appears in the UBEIF (Figure 9). The image of every other underwater object point appears in the UBOIF (Figure 8).

BIOOPTICAL CONCLUSIONS

Animals that have to cope with the consequences of refraction while looking into the water from the air are, for example, (1) facet-eyed insects living on the water surface, (2) piscivorous birds, and (3) amphibious mammals. In order to strike a prey or perceive the correct distance to a

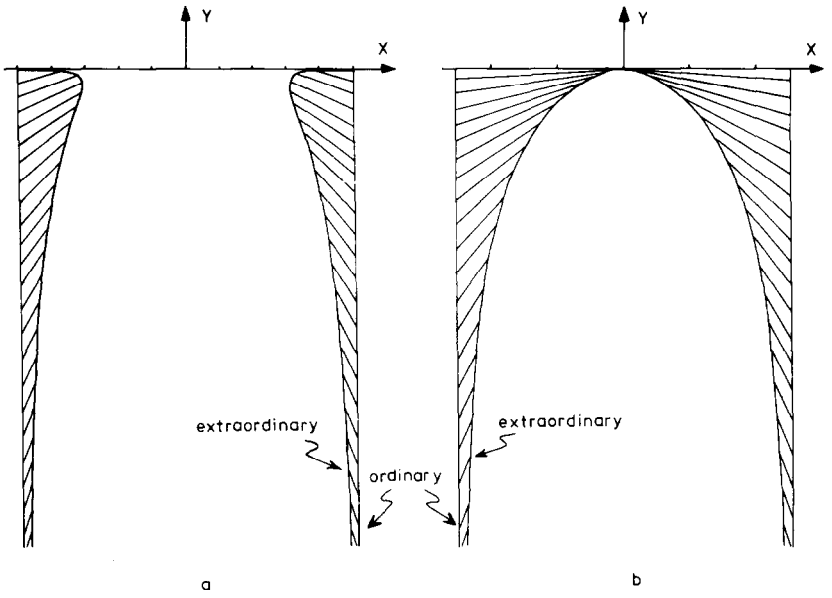

FIG. 11. The relationship between the UBOIF and the UBEIF as in Fig. 10 except that object points lie along a vertical underwater line.

predator, all these animals have to correct for refraction. A well-known representative of animals in group 1 is the waterstrider *Gerris*. Its underwater visual field is treated in [14]. The animals in group 2 frequently detect, locate, and start to seize an aquatic prey while the eyes are above water. This has been observed in pelicans (Pelecanidae), gannets, and boobies (Sulidae), ospreys (Pandionidae), terns (Laridae), and kingfishers (Alcedinidae), for example [8–12]. Since these animals keep their eyes in a horizontal plane, they will perceive an UBOIF. However, there is an exception. When an object comes to lie in a vertical plane across the eye, its image will be within the UBEIF provided that the animal has a binocular visual field in this plane. Usually, the attacked prey is in front of the predator, and hence within the UBOIF. Indeed, the profound investigations by Katzir and Intrator [6] and Katzir et al. [7] of the catching of submerged and nonsubmerged prey by the western reef heron *Egretta gularis schistacea* demonstrate that the visual system of this bird is adapted to precisely locate objects within the UBOIF. It would be interesting to test whether *Egretta* can also locate and seize a fish that lies in the vertical

plane across the eyes and thus within the UBEIF.

An example of animals in group 3 is the harbor seal *Phoca vitulina*. It is particularly interesting, because it can be observed to lie flat or on its side when it is ashore. The image of a submerged object can thus be within either the UBOIF or the UBEIF.

The visual tasks the seal is confronted with are manyfold. When submerged, it has to detect and locate prey. The bonding between mothers and the young and skittish offspring is eminently important. A pup less than 15 min old follows its mother into the water, where the level of ambient noise can be high. Thus, for maintaining contact between mother and pup, underwater vision might play an important role.

Also when resting ashore, the visual tracking of submerged objects is of considerable importance to a seal. Again, it has to watch its offspring, which might remain and be submerged in the water. It has also to detect visually its main predator, the polar bear, when it attacks from below the water surface.

The eye of the seal is well adapted to its amphibious habits [5]. The large and spherical lens is suited for underwater acuity; it compensates for the fact that the refractive indices of water and cornea are almost the same and consequently the cornea does not contribute substantially to image formation. In air the cornea is astigmatic; its curvature is not smooth, particularly along the equator of the eye. In water this astigmatism is of no disadvantage because the cornea does not refract the light. Vision on land is improved by means of a stenopaic pupil, which closes down to a vertical slit that is parallel to the axis of least astigmatism. When the pupil does not close—for example, on foggy or dimly lit beaches—the visual world of the seal is blurred. But when the light level is high enough, as it usually is near the sea or on ice, the stenopaic pupil compensates for astigmatism, and the seal's acuity may be as good in air as in water.

We turn now to the question of what consequences the resting position of a seal, flat or on the side, might have with respect to the tasks mentioned above. Just to recapitulate briefly, the image of an object within the UBOIF (animal lying flat) appears elevated although its apparent horizontal distance corresponds to its true position. However, when the image is within the UBEIF (animal lying on its side), its apparent horizontal distance is reduced, too.

It is important that a submerged pup must not move away from the mother beyond a critical distance or it will expose itself to danger. Lying on its side, the mother seal would underestimate the horizontal distance to the pup unless its visual system corrected for the distorted UBEIF. Otherwise it would be more advantageous to lie flat and keep the eyes in a horizontal plane.

Concerning a polar bear attacking from below the water surface, the situation is more complex. In this case the seal has to keep the distance to the predator beyond a critical value in order to have time for a safe escape. It appears, therefore, that lying on the side would be of advantage, since in this position the perceived distance is shorter than the true one. On the other hand, lying on the side is a less favorable starting position than lying flat. It is possible that the advantages of watching the image of a submerged enemy within the UBEIF is just compensated for by the less favorable starting position, and therefore when it comes to a successful escape the resting position does not matter.

We thank M. Carruthers for reading and correcting the manuscript. Financial support came from the Deutsche Forschungsgemeinschaft (SFB 307).

REFERENCES

1 L. Matthiessen, Das astigmatische Bild des horizontalen, ebenen Grundes eines Wasserbassins, *Ann. Phys.* 4(6):347 (1901).
2 L. E. Kinsler, Imaging of underwater objects, *Am. J. Phys.* 13(4) 255–257 (1945).
3 R. J. Schusterman, Behavioral capabilities of seals and sea lions: a review of their hearing, visual, learning and diving skills, *Physiol. Rec.* 31:125–143 (1981).
4 D. Renouf, J. Lawson, and L. Gaborko, Attachment between harbour seal (*Phoca vitulina*) mothers and pups, *J. Zool.* 199:179–187 (1983).
5 D. Renouf, Sensory function in the harbour seal, *Sci. Am.* 260(4):62–67 (1989).
6 G. Katzir and N. Intrator, Striking of underwater prey by a reef heron, *Egretta gularis schistacea*, *J. Comp. Physiol.* A160:517–523 (1987).
7 G. Katzir, A. Lotem, and N. Intrator, Stationary underwater prey missed by reef herons, *Egretta gularis*: head position and light refraction at the moment of strike, *J. Comp. Physiol.* A165:573–576 (1989).
8 G. W. Salt, and D. O. Willard, The hunting behaviour and success of Forster's tern, *Ecology* 52:989–998 (1981).
9 F. G. Buckley and P. A. Buckley, Comparative feeding ecology of wintering adult and juvenile royal terns (Aves: Laridae, Sterninae), *Ecology* 55:1053–1063 (1974).
10 R. J. Douthwaite, Fishing techniques and foods of the pied kingfisher on lake Victoria, *Ostrich* 47:153–160 (1976).
11 M. P. Harris, Unusual feeding by the blue footed booby, *Auk* 92:601–602 (1975).
12 R. W. Schreiber, G. E. Woolfenden, and W. E. Curtsinger, Prey capture by the brown Pelican, *Auk* 92:649–654 (1974).
13 L. J. Milne and M. Milne, Insects of the water surface, *Sci. Am.* 238(4):134–142 (1978).
14 D. Varjú and G. Horváth, Looking into the water with a facet eye, *Biol. Cybern.* 62:157–165 (1989).
15 G. Horváth and D. Varjú, On the structure of the aerial visual field of aquatic animals distorted by refraction, *Bull. Math. Biol.* (in press).